On Channel Sharing Policies in LEO Mobile Satellite Systems

IOANNIS D. MOSCHOLIOS
University of Peloponnese, Tripolis, Greece

VASSILIOS G. VASSILAKIS
University of York, York, U.K.

NIKOS C. SAGIAS, Senior Member, IEEE
University of Peloponnese, Tripolis, Greece

MICHAEL D. LOGOTHETIS, Senior Member, IEEE
University of Patras, Patras, Greece

We consider a low earth orbit (LEO) mobile satellite system with "satellite-fixed" cells that accommodates new and handover calls of different service-classes. We provide an analytical framework for the efficient calculation of call blocking and handover failure probabilities under two channel sharing policies, namely the fixed channel reservation and the threshold call admission policies. Simulation results verify the accuracy of the proposed formulas. Furthermore, we discuss the applicability of the policies in software-defined LEO satellites.

Manuscript received February 3, 2017; revised August 10, 2017; released for publication November 28, 2017. Date of publication January 25, 2018; date of current version August 7, 2018.

DOI. No. 10.1109/TAES.2018.2798318

Refereeing of this contribution was handled by T J. Willink.

Authors' addresses: I. D. Moscholios and N. C. Sagias are with the Department of Informatics & Telecommunications, University of Peloponnese, Tripolis 221 31, Greece, E-mail: (idm@uop.gr; nsagias@uop.gr). V. G. Vassilakis is with the Department of Computer Science, University of York, York YO10 5GH, U.K. E-mail: (vasileios.vasilakis@york.ac.uk). M. D. Logothetis is with the Department of Electrical & Computer Engineering, University of Patras, Patras 265 04, Greece, E-mail: (mlogo@upatras.gr). Corresponding author is Ioannis D. Moscholios, E-mail: (idm@uop.gr).

I. INTRODUCTION

Low earth orbit (LEO) mobile satellite systems (MSS) are ideally suited for globally providing multiservice real time applications to a diverse population [1]. Compared to geostationary earth orbit satellite systems, their requirements in terms of transmit power and transmission delays are significantly lower at the expense of frequent beam handovers (that occur due to the high speed of LEO satellites) to in-service mobile users (MUs).To assure a high quality of service (QoS) in the complicated multirate traffic environment of contemporary LEO-MSS, it is essential to develop QoS mechanisms, with efficient and fast QoS assessment, that:

1) provide access to the bandwidth needed by the services of the MUs,
2) ensure fairness among different "competing" mobile services/applications, and
3) reduce handover failures for in-service MUs.

On the other hand, the incorporation of the emerging technologies of software-defined networking (SDN) and network function virtualization (NFV) in next-generation satellite networks [2], [3], provides new opportunities for fairer QoS assignment among service classes. SDN decouples the control plane from the data plane, while NFV abstracts the network functions from the underlying physical infrastructure. SDN and NFV, although not dependent on each other, are closely related and complementary concepts.

Considering call-level traffic in a LEO-MSS which accommodates different service-classes with different QoS requirements, a QoS mechanism that affects call-level performance measures, such as call blocking probabilities (CBP) and handover failure probabilities, is a channel sharing policy. The QoS assessment of LEO-MSS under a channel sharing policy can be accomplished through teletraffic loss or queuing models. In the literature, there are various teletraffic loss or queuing models that describe channel sharing policies in LEO-MSS [4]–[17]. Although there are different ways to classify them, e.g., in terms of the channel sharing policy, the call arrival process, the existence of queues or not etc., for presentation purposes, we classify them in two categories: 1) single-rate [4]–[13] and 2) multirate [14]–[17] models.

By considering the first category, in [4], each cell is modeled as a Markovian loss-queuing model that accommodates Poisson calls (new or handover) that require a single channel in order to be accepted in the cell. To guarantee a certain QoS to handover calls, a fixed channel reservation (FCR) policy is considered, named channel-locking mechanism, that treats different the first handover from the subsequent handovers of a call. Extensions of [4] are related to schemes based on the following:

1) dynamic channel reservation with [5] or without priorities [6];
2) time-based channel reservation [7], [8];
3) Doppler-based handover prioritization [9], [10];

4) probabilistic reservation for the handover management [11]; and
5) FCR with first-in-first-out queuing handover [12].

Recently, in [13], a queueing model has been proposed for the analysis of a LEO-MSS in the case of correlated service times.

By considering the second category, in [14], an analytical framework is proposed for the performance evaluation of LEO-MSS with "satellite-fixed" cells accommodating multirate Poisson traffic under the complete sharing (CS) and the FCR policies. Under the CS policy, all calls have access to all available channels. A call is accepted in a cell whenever the required channels are available; otherwise, call blocking occurs. Contrary to the FCR policy, the CS policy is unfair to calls with higher channel requirements since it results in higher CBP. In [15], in addition to the CS and the FCR policies, the complete partitioning (CP) and the threshold call admission (TCA) policies are proposed. In the CP policy, the capacity C (in channels) of a cell is partitioned into K subsets, where K is the number of service-classes accommodated in the cell. By assuming that each partition k ($k = 1, \ldots, K$) has a capacity C_k and belongs to calls of service-class k, each cell can be modeled as an $M/M/C_k/C_k$ system. However, since the CP policy can lead to poor channel utilization we do not consider it herein. The interested reader may also resort to [16] for an analysis on optimum CP policies. In the TCA policy, a new service-class k call is not accepted in a cell if the number of in-service new and handover service-class k calls plus the new call exceeds a threshold (different for each service-class). In [15], simulation results initially are presented for the TCA policy, while in [17], an analytical Markovian model is proposed that allows the determination of the performance measures by solving the global balance (GB) equations of K-dimensional Markov chains. This task is computationally extremely complex (if not impossible) and time consuming for systems with large capacities and many service-classes, since it requires the solution of a linear system of millions or even billions of GB equations. A similar complex procedure (based on solving a linear system of GB equations) is proposed in the case of the FCR policy in [14] and [15].

In both categories, in-service calls have a fixed channel assignment. The case of elastic calls whose channel requirements can tolerate compression has not been studied in LEO-MSS. A possible springboard for such an analysis can be the works of [18]–[22] whereby loss/queueing models are proposed for wired [18]–[20] or wireless [21], [22] networks under different channel sharing policies.

In this paper, we provide simple and yet efficient formulas for the calculation of various performance measures under the FCR and the TCA policies. These formulas significantly reduce the computational complexity, and therefore, can be invoked in network planning and dimensioning procedures. In addition, they provide highly accurate results as compared to equivalent simulation ones. Our contribution is threefold.

1) We propose a recursive formula for the calculation of the channel occupancy distribution in the case of the FCR policy. Compared to [14], [15] where enumeration and processing of the state-space is required (an extremely complex procedure for systems of large capacity and many service-classes), the proposed formula has a low computational complexity of $O(KC)$.
2) We show that: a) the steady-state probability distribution in the TCA has a product form solution (PFS), and b) the channel occupancy distribution can be easily determined with the aid of a convolution algorithm. Compared to [17], where again enumeration and processing of the state-space is required, the proposed algorithm has a low computational complexity of $O(KC^2)$.
3) Provide a framework for the applicability of the proposed models in LEO SDN/NFV satellite networks. The evolution of such networks is expected to be the necessary step for the integration and operation of combined SDN/NFV satellite and terrestrial networks.

The remainder of this paper is as follows: In Section II, we present the LEO MSS model under consideration, in detail. In Section II-A, we provide a description of the model, in Section II-B, we determine the handover arrival rate and the channel holding time while in Section II-C, we provide insight to the analytical model under the CS policy. In Section III, we show a recursive formula for the calculation of the channel occupancy distribution in the case of the FCR policy. In Section IV, we show that the TCA policy has a PFS and provide a convolution algorithm for the calculation of the channel occupancy distribution and consequently all performance measures. In Section V, we discuss the applicability of the proposed models in LEO SDN/NFV satellite networks. In Section VI, we present analytical and simulation results for various performance measures, for evaluation, while in Section VII, we present the conclusion. For the reader's convenience, Table I includes the list of abbreviations used in this paper.

II. LEO-MSS MODEL

A. Description

Adopting the model of [15], we consider a LEO-MSS of N contiguous "satellite-fixed" cells, each modeled as a rectangle of length L (425 km in the case of the Iridium LEO-MSS [23]), that form a strip of contiguous coverage on the region of the Earth. Each cell has a fixed capacity of C channels. The system of these N cells accommodates MUs who generate calls of K service-classes with different QoS requirements. Each service-class k ($k = 1, \ldots, K$) call requires a fixed number of b_k channels for its whole duration in the system. New and handover calls of service-class k follow a Poisson process with arrival rates λ_k and λ_{hk}, respectively. New calls may arrive in any cell with equal probability (i.e., it is assumed that MUs are uniformly distributed in the system of cells). The cell that a new call originates is the source cell. The arrival of handover calls in a cell is as follows: Handover calls cross the source cell's

TABLE I
List of Abbreviations

CBP	Call blocking probabilities
CP	Complete partitioning
cRRM	Centralized radio resource management
CS	Complete sharing
dRRM	Distributed radio resource management
FCR	Fixed channel reservation
GB	Global balance
LB	Local balance
LEO	Low earth orbit
MSS	Mobile satellite system
MU	Mobile user
NCC	Network control center
NFV	Network function virtualization
NFVI	Network function virtualization infrastructure
NMC	Network management center
PFS	Product form solution
PoP	Point of presence
QoS	Quality of service
RRM	Radio resource management
SDN	Software-defined networking
SNO	Satellite network operator
ST	Satellite terminal
TCA	Threshold call admission
VMM	Virtual machine monitor
VNF	Virtual network function
VSNO	Virtual satellite network operator

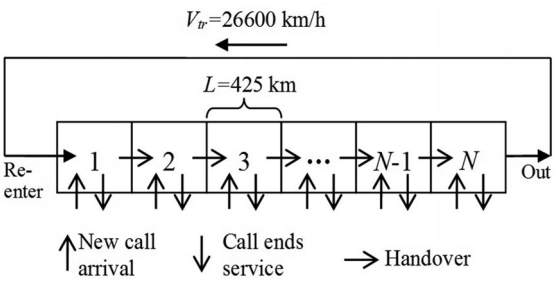

Fig. 1. Rectangular cell model for the LEO-MSS network.

boundaries to the adjacent right cell having a velocity of $-V_{tr}$, where V_{tr} (approx. 26600 km/h in the Iridium constellation) is the subsatellite point speed (see Fig. 1). This assumption is valid as long as the rotation of the Earth and the speed of an MU are negligible compared to the subsatellite point speed on the Earth [4]. An in-service call that departs from cell N (the last cell) requests a handover in cell 1, thus having a continuous cellular network (see Fig. 1).

Based on the above, let t_c be the dwell (or sojourn) time of a call in a cell. Then, t_c is: (i) uniformly distributed in $[0, L/V_{tr}]$ for new calls in their source cell and (ii) deterministically equal to $T_c = L/V_{tr}$ for handover calls that traverse, from border to border, any adjacent cell. Based on (ii), T_c expresses the interarrival time for all handovers subsequent to the first one. The duration of a service-class k call (new or handover) in the system and the channel holding time in a cell are exponentially distributed with mean T_{dk} and μ_k^{-1}, respectively.

B. Determination of Handover Arrival Rate and Channel Holding Time

To determine formulas for the handover arrival rate λ_{hk} and the channel holding time with mean μ_k^{-1} of service-class k calls, some necessary definitions are required as follows.

1) The (dimensionless) parameter γ_k, which is the ratio between the mean duration of a service-class k call in the system and the dwell time of a call in a cell [4]

$$\gamma_k = T_{dk}/T_c. \tag{1}$$

Note that this parameter expresses the average number of handover requests per service-class k call assuming that there is no blocking.

2) The time $T_{h1,k}$, which expresses the interval from the arrival of a new service-class k call in the source cell to the instant of the first handover. $T_{h1,k}$ is uniformly distributed in $[0, T_c]$ with probability density function (pdf) [24]

$$\text{pdf}_{T_{h1,k}}(t) = \begin{cases} \dfrac{V_{tr}}{L}, & \text{for } 0 \le t \le \dfrac{1}{\gamma_k} T_{dk} \\ 0, & \text{otherwise} \end{cases}. \tag{2}$$

3) The probabilities $P_{h1,k}$ and $P_{h2,k}$, which express the handover probability for a service-class k call in the source cell and in a transit cell, respectively. Due to the different distances covered by an MU in the source cell and in the transit cells, these probabilities are different. More precisely, $P_{h1,k}$ is defined as

$$\begin{aligned} P_{h1,k} &= \int_0^\infty \Pr\{t_{dk} > t | T_{h1,k} = t\} \text{pdf}_{T_{h1,k}}(t) dt \\ &= \int_0^\infty e^{-t/T_{dk}} \text{pdf}_{T_{h1,k}}(t) dt = \gamma_k (1 - e^{-(1/\gamma_k)}) \end{aligned} \tag{3}$$

where t_{dk} is the service-class k call duration time (exponentially distributed with mean T_{dk}). The residual service time of a service-class k call after a successful handover request has the same pdf as t_{dk} (due to the memoryless property of the exponential distribution [25]). It follows then that $P_{h2,k}$ can be expressed by

$$\begin{aligned} P_{h2,k} &= \Pr\left\{t_{dk} > \frac{L}{V_{tr}}\right\} = 1 - \Pr\left\{t_{dk} \le \frac{L}{V_{tr}}\right\} \\ &= 1 - \int_0^{T_c} \frac{1}{T_{dk}} e^{-t/T_{dk}} dt = e^{-(1/\gamma_k)}. \end{aligned} \tag{4}$$

The handover arrival rate λ_{hk} can be related to λ_k by assuming that in each cell there exists a flow equilibrium between MUs entering and MUs leaving the cell. In that case, we may write the following flow equilibrium equation (MUs entering the cell = MUs leaving the cell)

$$\begin{aligned} &\lambda_k(1-P_{b_k})+\lambda_{hk}(1-P_{f_k}) \\ &=\lambda_{hk}+\lambda_k(1-P_{b_k})(1-P_{h1,k})+\lambda_{hk}(1-P_{f_k})(1-P_{h2,k}) \end{aligned} \tag{5}$$

where P_{b_k} refers to the CBP of new service-class k calls in the source cell and P_{f_k} refers to the handover failure prob-

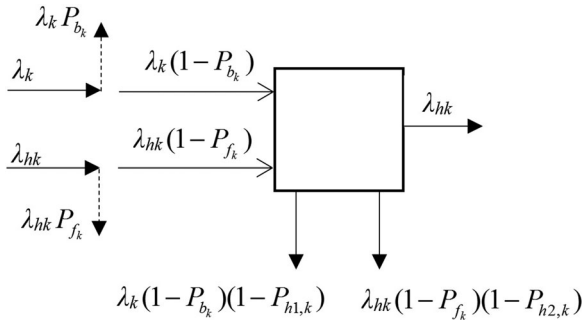

Fig. 2. Flow equilibrium of service-class k calls in a cell.

ability of service-class k calls in transit cells. The values of P_{b_k} and P_{f_k} will be determined in the following section.

The left-hand side of (5) refers to new and handover service-class k calls that are accepted in the cell with probability $(1 - P_{b_k})$ and $(1 - P_{f_k})$, respectively. The right-hand side of (5) refers to

1) calls that are handed over to the transit cell (1st term),
2) new calls that complete their service in the source cell (2nd term), and
3) handover calls that do not handover to the transit cell (3rd term).

A graphical representation of (5) is given in Fig. 2. Equation (5), can be rewritten as

$$\frac{\lambda_{hk}}{\lambda_k} = \frac{(1 - P_{b_k})P_{h1,k}}{1 - (1 - P_{f_k})P_{h2,k}}. \tag{6}$$

To derive a formula for the channel holding time of service-class k calls, we remind that channels are occupied either: 1) by new or handover calls and 2) until the end of service of a call or until a call is handed over to a transit cell. Since the channel holding time can be expressed as $t_{h1,k} = \min(t_{dk}, t_c)$ in the case of the source cell and $t_{h2,k} = \min(t_{dk}, T_c)$ in the case of a transit cell, then the mean value of $t_{hi,k}$, $E_k(t_{hi,k})$ for $i = 1, 2$ is given by [15]

$$E_k(t_{hi,k}) = T_{dk}(1 - P_{hi,k}). \tag{7}$$

We define now by P_k and P_k^h the probabilities that a channel is occupied by a new and a handover service-class k call, respectively. Then

$$P_k = \frac{\lambda_k(1 - P_{b_k})}{\lambda_k(1 - P_{b_k}) + \lambda_{hk}(1 - P_{f_k})} \tag{8}$$

and

$$P_k^h = \frac{\lambda_{hk}(1 - P_{f_k})}{\lambda_k(1 - P_{b_k}) + \lambda_{hk}(1 - P_{f_k})}. \tag{9}$$

Based on (7)–(9), the channel holding time of service-class k calls (either new or handover) is approximated by an exponential distribution whose mean μ_k^{-1} is the weighted sum of (7) (for $i = 1, 2$) multiplied by the corresponding probabilities P_k (for $i = 1$) and P_k^h (for $i = 2$)

$$\begin{aligned}\mu_k^{-1} &= P_k E_k(t_{h1,k}) + P_k^h E_k(t_{h2,k}) \\ &= \frac{\lambda_k(1 - P_{b_k})E_k(t_{h1,k})}{\lambda_k(1 - P_{b_k}) + \lambda_{hk}(1 - P_{f_k})} \\ &\quad + \frac{\lambda_{hk}(1 - P_{f_k})E_k(t_{h2,k})}{\lambda_k(1 - P_{b_k}) + \lambda_{hk}(1 - P_{f_k})}.\end{aligned} \tag{10}$$

C. Analytical LEO-MSS Model Based on the CS Policy

To analyze the LEO-MSS, each cell is modeled as a multirate loss system whereby the available channels are shared according to the CS policy. The CS policy is the springboard for the analysis of more complicated channel sharing policies and, therefore, an insight to this policy is essential for presentation purposes.

To this end, let the system be in steady state and denote by n_k the number of in-service calls (new or handover) of service-class k in a cell. Then, the steady-state vector is defined as $\boldsymbol{n} = (n_1, \ldots, n_k, \ldots, n_K)$ and its corresponding probability distribution as $P(\boldsymbol{n})$. By exploiting local balance (LB) between the adjacent states: $\boldsymbol{n_k^-} = (n_1, \ldots, n_k - 1, \ldots, n_K)$ and $\boldsymbol{n} = (n_1, \ldots, n_k, \ldots, n_K)$, the values of $P(\boldsymbol{n})$ are given by the PFS

$$P(\boldsymbol{n}) = G^{-1}\left(\prod_{k=1}^{K} \frac{\alpha_k^{n_k}}{n_k!}\right) \tag{11}$$

where G is the normalization constant given by

$$G \equiv G(\boldsymbol{\Omega}) = \sum_{\boldsymbol{n}\in\boldsymbol{\Omega}} \left(\prod_{k=1}^{K} \frac{\alpha_k^{n_k}}{n_k!}\right) \tag{12}$$

where $\boldsymbol{\Omega}$ is the state space of the system, $\boldsymbol{\Omega} = \{\boldsymbol{n} : 0 \le \boldsymbol{nb} \le C, k = 1, \ldots, K\}$, $\boldsymbol{nb} = \sum_{k=1}^{K} n_k b_k$, $\boldsymbol{b} = (b_1, \ldots, b_K)^T$ and $\alpha_k = (\lambda_k + \lambda_{hk})/\mu_k$ is the offered traffic-load (in erl) of service-class k calls in a cell.

A new service-class k call is blocked and lost if the required b_k channels are not available in the cell upon its arrival. Based on (11), we determine CBP of new service-class k calls, P_{b_k}, via the formula

$$P_{b_k} = 1 - \sum_{\boldsymbol{n}\in\boldsymbol{\Omega_k}} P(\boldsymbol{n}) \tag{13}$$

where $\boldsymbol{\Omega_k} = \{\boldsymbol{n} : 0 \le \boldsymbol{nb} \le C - b_k, k = 1, \ldots, K\}$.

Equation (13) has a computational complexity in the order of $O(C^K)$ a fact that makes it impractical for real systems of large capacities and many service-classes. To substantially reduce the complexity to O(CK), let j be the number of occupied channels in the cell, i.e., $j = \sum_{k=1}^{K} n_k b_k$, $j = 0, 1, \ldots, C$. Then, the following recursive formula is proposed for the calculation of the channel occupancy distribution $q(j)$ [15]

$$q(j) = \begin{cases} 1, & \text{for } j = 0 \\ \frac{1}{j}\displaystyle\sum_{k=1}^{K} \alpha_k b_k q(j - b_k), & \text{for } j = 1, \ldots, C \\ 0, & \text{otherwise} \end{cases} \tag{14}$$

which is the classical Kaufman–Roberts formula [26], [27].

Based on (14), the values of P_{b_k} are given by

$$P_{b_k} = \sum_{j=C-b_k+1}^{C} G^{-1} q(j) \tag{15}$$

where $G = \sum_{j=0}^{C} q(j)$ is the normalization constant.

Since the CS policy does not prioritize handover calls, we assume that

$$P_{f_k} = P_{b_k}. \tag{16}$$

Equation (16) is further modified to take into account the successive handovers of a call during its service in the system

$$P_{f_k} = \delta_k P_{b_k} \tag{17}$$

where δ_k is a correction factor introduced to model the dependency between successful handovers of a service-class k call prior to a handover failure. The latter may occur during the $E_k(n_{hk})$th handover if an accepted call has already performed $E_k(n_{hk}) - 1$ successful handovers, i.e.,

$$\delta_k = (1 - P_{b_k}) P_{h1,k} (1 - P_{f_k})^{E_k(n_{hk})-2} P_{h2,k}^{E_k(n_{hk})-2} \tag{18}$$

where $E_k(n_{hk})$ is the average number of times that a new service-class k call is successfully handed over during its lifetime in the system (for the proof see Appendix A)

$$E_k(n_{hk}) = \frac{(1 - P_{b_k}) P_{h1,k}}{1 - (1 - P_{f_k}) P_{h2,k}}. \tag{19}$$

To determine $q(j)$'s, P_{b_k}, and P_{f_k} via (15)–(18), the values of offered traffic-load of each service-class k, $\alpha_k = (\lambda_k + \lambda_{hk})/\mu_k$, are required. Since λ_{hk} and μ_k^{-1} depend on P_{b_k} and P_{f_k} [see (6) and (10)] an iterative procedure is necessary. The latter starts with $P_{b_k} = 0$ and stops when two consecutive values of P_{b_k} differ by less than 10^{-6} [15].

Having calculated $q(j)$'s, P_{b_k}, and P_{f_k} the following performance measures can be determined.

1) The call dropping probability of service-class k calls, P_{d_k}, which refers to new calls that are not blocked, but are forced to terminate due to handover failure

$$P_{d_k} = \frac{P_{f_k} P_{h1,k}}{1 - (1 - P_{f_k}) P_{h2,k}}. \tag{20}$$

2) The unsuccessful call probability of service-class k calls, P_{us_k}, which refers to calls that are either blocked in the source cell or dropped due to a handover failure

$$P_{us_k} = P_{b_k} + P_{d_k}(1 - P_{b_k}). \tag{21}$$

III. PROPOSED RECURSIVE FORMULA FOR THE LEO-MSS MODEL BASED ON THE FCR POLICY

To facilitate the description of the analytical model under the FCR policy, we distinguish new from handover calls and assume that each cell accommodates calls of $2K$ service-classes. A service-class k call is new if $1 \le k \le K$ and handover if $K + 1 \le k \le 2K$.

The FCR policy is described as follows. A call of service class k ($k = 1, \ldots, 2K$) requests b_k channels and has an FCR parameter CR_k that expresses the integer number of channels reserved to benefit calls of all other service-classes except from k. The analysis presented herein is more general as compared to [15] since it allows the application of the FCR policy to all calls (new or handover) of a service-class k. In that sense, the FCR policy can be applied to favor handover calls of a service-class against new or handover calls from other service-classes. In [15], the FCR policy benefits only handover calls of a service-class against new calls from other service-classes.

The GB equation for state $\boldsymbol{n} = (n_1, \ldots, n_k, \ldots, n_{2K})$, expressed as *rate into state* $\boldsymbol{n}$ = *rate out of state* $\boldsymbol{n}$, is given by

$$\begin{aligned} \sum_{k=1}^{K} \lambda_k(\boldsymbol{n}_k^-) P(\boldsymbol{n}_k^-) + \sum_{k=K+1}^{2K} \lambda_{kh}(\boldsymbol{n}_k^-) P(\boldsymbol{n}_k^-) \\ + \sum_{k=1}^{2K} (n_k + 1) \mu_k P(\boldsymbol{n}_k^+) = \sum_{k=1}^{K} \lambda_k(\boldsymbol{n}) P(\boldsymbol{n}) \\ + \sum_{k=K+1}^{2K} \lambda_{kh}(\boldsymbol{n}) P(\boldsymbol{n}) + \sum_{k=1}^{2K} n_k \mu_k P(\boldsymbol{n}) \end{aligned} \tag{22}$$

where

$$\lambda_k(\boldsymbol{n}) = \begin{cases} \lambda_k, & \text{for } C - \boldsymbol{n}\boldsymbol{b} \ge b_k + CR_k \\ 0, & \text{otherwise} \end{cases} \tag{23}$$

$$\lambda_{kh}(\boldsymbol{n}) = \begin{cases} \lambda_{kh}, & \text{for } C - \boldsymbol{n}\boldsymbol{b} \ge b_k + CR_k \\ 0, & \text{otherwise} \end{cases} \tag{24}$$

$\boldsymbol{n}_k^- = (n_1, \ldots, n_k - 1, \ldots, n_{2K})$, $\boldsymbol{n}_k^+ = (n_1, \ldots, n_k + 1, \ldots, n_{2K})$ and $P(\boldsymbol{n})$, $P(\boldsymbol{n}_k^-)$, $P(\boldsymbol{n}_k^+)$ are the probability distributions of states $\boldsymbol{n}$, $\boldsymbol{n}_k^-$, $\boldsymbol{n}_k^+$, respectively.

The FCR model does not have a PFS for the determination of the steady-state probabilities $P(\boldsymbol{n})$ since LB can be destroyed between adjacent states $\boldsymbol{n}_k^-$, $\boldsymbol{n}$ or $\boldsymbol{n}$, $\boldsymbol{n}_k^+$ due to the existence of the FCR parameters. This means that $P(\boldsymbol{n})$'s (and consequently all performance measures) can be determined by solving the set of linear GBs, a realistic task only for cells of very small capacity and two or three service-classes.

Contrary to [14], [15], where it is suggested to apply a linear equation procedure (such as the Gauss-Siedel iteration) for solving the GBs, we prove an approximate, but recursive formula for the calculation of the occupancy distribution, $q(j)$, of the FCR model (see Appendix B for the proof)

$$q(j) = \begin{cases} 1, & \text{for } j = 0 \\ \frac{1}{j} \sum_{k=1}^{2K} \alpha_k (j - b_k) b_k q(j - b_k), & \text{for } j = 1, \ldots, C \\ 0, & \text{otherwise} \end{cases} \cdot \tag{25}$$

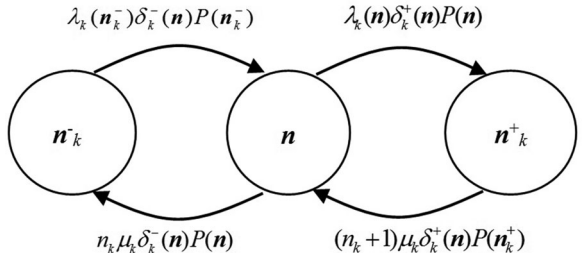

Fig. 3. State transition diagram between adjacent states of the TCA model for service-class k.

Based on (25), the values of P_{b_k} $(k = 1, \ldots, K)$ are given by

$$P_{b_k} = \sum_{j=C-b_k-CR_k+1}^{C} G^{-1}q(j) \tag{26}$$

where $G = \sum_{j=0}^{C} q(j)$ is the normalization constant.

Similarly, the values of $P_{f_k}(k = K+1, \ldots, 2K)$ are given by

$$P_{f_k} = \delta_k \sum_{j=C-b_k-CR_k+1}^{C} G^{-1}q(j) \tag{27}$$

where the factor δ_k is given by (18).

As far as the values of P_{d_k} and P_{us_k} are concerned, they can be calculated via (20) and (21), respectively.

IV. PROPOSED CONVOLUTION ALGORITHM FOR THE LEO-MSS MODEL BASED ON THE TCA POLICY

In the TCA policy, a threshold N_k is defined for each service-class k that denotes the maximum number of new and handover in-service calls of service-class k that are allowed in a cell. Due to this definition, we do not distinguish new from handover calls and assume that each cell accommodates calls of K service-classes.

The TCA policy is applied only to new service-class k calls. More precisely, a new service-class k call is accepted in a cell if and only if: 1) there exist available channels, i.e., $j + b_k \leq C$ and 2) the number of new and handover in-service calls of service-class k plus the new one does not exceed the threshold N_k, i.e., $n_k + 1 \leq N_k$. The last restriction shows that a new call may not be accepted in the cell even if available channels do exist. On the other hand, a handover service-class k call is accepted in a transit cell if and only if $j + b_k \leq C$.

Contrary to [15], where only simulation results are presented in the case of the TCA policy, or [17] where the set of GB equations should be solved, we propose the mathematical framework for the efficient calculation of all relevant performance measures.

To this end, let the system be in steady state and define the steady-state vector as $\boldsymbol{n} = (n_1, \ldots n_k, \ldots n_K)$ and its corresponding probability distribution as $P(\boldsymbol{n})$.

Based on the state transition diagram of the TCA model (see Fig. 3), the GB equation for state $\boldsymbol{n}$, expressed as *rate into state* $\boldsymbol{n}$ = *rate out of state* $\boldsymbol{n}$, is

$$\sum_{k=1}^{K}\lambda_k(\boldsymbol{n}_k^-)\delta_k^-(\boldsymbol{n})P(\boldsymbol{n}_k^-) + \sum_{k=1}^{K}(n_k+1)\mu_k\delta_k^+(\boldsymbol{n})P(\boldsymbol{n}_k^+)$$
$$= \sum_{k=1}^{K}\lambda_k(\boldsymbol{n})\delta_k^+(\boldsymbol{n})P(\boldsymbol{n}) + \sum_{k=1}^{K}n_k\mu_k\delta_k^-(\boldsymbol{n})P(\boldsymbol{n}) \tag{28}$$

where $\lambda_k(\boldsymbol{n}) = \begin{cases} \lambda_k + \lambda_{kh}, \text{if } n_k \leq N_k \\ \lambda_{kh}, \text{if } n_k > N_k \end{cases}$, $\delta_k^+(\boldsymbol{n}) = \begin{cases} 1, \text{if } \boldsymbol{n}_k^+ \in \boldsymbol{\Omega} \\ 0, \text{otherwise} \end{cases}$, $\delta_k^-(\boldsymbol{n}) = \begin{cases} 1, \text{if } \boldsymbol{n}_k^- \in \boldsymbol{\Omega} \\ 0, \text{otherwise} \end{cases}$, $\boldsymbol{\Omega} = \{\boldsymbol{n} : 0 \leq \boldsymbol{nb} \leq C, n_k \leq N_k, k = 1, \ldots, K\}$ and $\boldsymbol{nb} = \sum_{k=1}^{K} n_k b_k$, $\boldsymbol{b} = (b_1, \ldots, b_K)^T$.

According to Fig. 3, the corresponding Markov chain of the TCA model retains reversibility due to the so-called Kolmogorov's criterion [25]: The circulation flow among four adjacent states equals zero: Flow clockwise = Flow counter-clockwise. Because of this, LB exists between adjacent states and the following LB equations are extracted as (*rate up* = *rate down*), for $k = 1, \ldots, K$ and $\boldsymbol{n} \in \boldsymbol{\Omega}$

$$\lambda_k(\boldsymbol{n}_k^-)\delta_k^-(\boldsymbol{n})P(\boldsymbol{n}_k^-) = n_k\mu_k\delta_k^-(\boldsymbol{n})P(\boldsymbol{n}) \tag{29}$$
$$\lambda_k(\boldsymbol{n})\delta_k^+(\boldsymbol{n})P(\boldsymbol{n}) = (n_k+1)\mu_k\delta_k^+(\boldsymbol{n})P(\boldsymbol{n}_k^+). \tag{30}$$

Based on the existence of LB, the probability distribution $P(\boldsymbol{n})$ of the TCA model can be described by the PFS

$$P(\boldsymbol{n}) = G^{-1}\left(\prod_{k=1}^{K}\frac{x_k^{n_k}}{n_k!}\right) \tag{31}$$

with $\frac{x_k^{n_k}}{n_k!} = \begin{cases} \frac{\alpha_k^{n_k}}{n_k!} \text{ if } n_k \leq N_k \\ \frac{\alpha_{kn}^{N_k}\alpha_{kh}^{(n_k-N_k)}}{n_k!} \text{ if } n_k > N_k \end{cases}$ and $G = \sum_{\boldsymbol{n}\in\boldsymbol{\Omega}}\left(\prod_{k=1}^{K}\frac{x_k^{n_k}}{n_k!}\right)$, $\alpha_k = (\lambda_k + \lambda_{kh})/\mu_k = \alpha_{kn} + \alpha_{kh}$, $\alpha_{kn} = \lambda_k/\mu_k$, $\alpha_{kh} = \lambda_{k,h}/\mu_k$.

For an efficient calculation of the various performance measures, we can exploit the PFS of the TCA model, and use the following three-step convolution algorithm.

Step 1: Determine the channel occupancy distribution $q_k(j)$ of each service-class k $(k = 1, \ldots, K)$, assuming that only service-class k exists in the system

$$q_k(j) = \begin{cases} \frac{q_k(0)\alpha_k^{n_k}}{n_k!} \text{ for } n_k \leq N_k \text{ and } j = n_k b_k \\ \frac{q_k(0)\alpha_{kn}^{N_k}\alpha_{kh}^{(n_k-N_k)}}{n_k!} \text{ for } n_k > N_k \text{ and } j = n_k b_k \end{cases}. \tag{32}$$

Step 2: Determine the aggregated occupancy distribution $Q_{(-k)}$ based on the successive convolution of all service-classes apart from service-class k

$$Q_{(-k)} = q_1 * \cdots * q_{k-1} * q_{k+1} * \cdots * q_K. \tag{33}$$

By the term "successive" we mean that initially q_1 and q_2 should be convolved to obtain q_{12}. Then, we convolve q_{12} with q_3 to obtain q_{123} etc. The convolution operation between two occupancy distributions of service-class k and

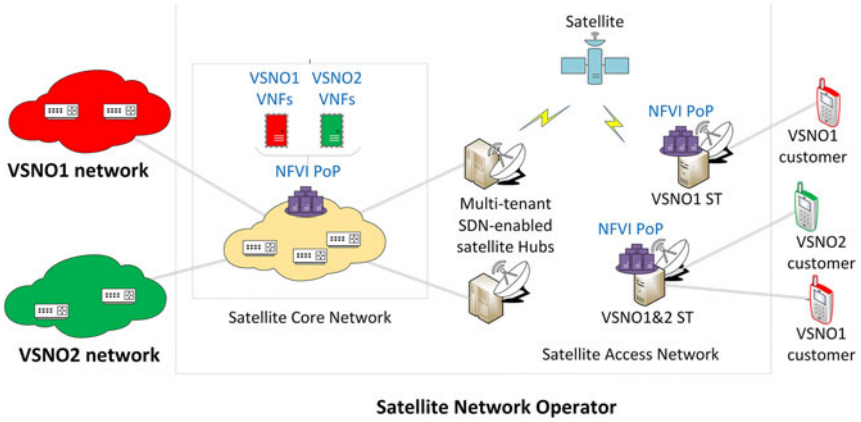

Fig. 4. SDN/NFV enabled satellite network architecture.

r is defined as

$$q_k * q_r = \Big\{ q_k(0)q_r(0), \sum_{m=0}^{1} q_k(m)q_r(1-m), \times \ldots, \sum_{m=0}^{C} q_k(m)q_r(C-m) \Big\}. \quad (34)$$

Step 3: Calculate the CBP of service-class k based on the convolution operation of $Q_{(-k)}$ (step 2) and q_k (see step 1) as

$$Q_{(-k)} * q_k = \Big\{ Q_{(-k)}(0)q_k(0), \sum_{m=0}^{1} Q_{(-k)}(m)q_k(1-m) \times \ldots, \sum_{m=0}^{C} Q_{(-k)}(m)q_k(C-m) \Big\}. \quad (35)$$

Normalizing the values of (35), we obtain the occupancy distribution $q(j)$, $j = 0, 1, \ldots, C$ via

$$q(0) = Q_{(-k)}(0)q_k(0)/G$$
$$q(j) = \Big(\sum_{m=0}^{j} Q_{(-k)}(m)q_k(j-m) \Big) \Big/ G, \; j = 1, \ldots, C. \quad (36)$$

Based on $q(j)$'s, we propose the following formula for the CBP of service-class k

$$P_{b_k} = \sum_{j=C-b_k+1}^{C} q(j) + \sum_{x=N_k b_k}^{C-b_k} q_k(x) \sum_{y=x}^{C-b_k} Q_{(-k)}(C-b_k-y). \quad (37)$$

The first term of (37) expresses those states j where there are no available channels for service-class k calls. The second term refers to states $x = N_k b_k, \ldots, C - b_k$ where there are available channels for calls, but call blocking occurs (for new calls) due to the TCA policy and the threshold N_k.

Similarly, the values of P_{f_k} can be determined via

$$P_{f_k} = \delta_k \Bigg[\sum_{j=C-b_k+1}^{C} q(j) + \sum_{x=N_k b_k}^{C-b_k} q_k(x) \times \sum_{y=x}^{C-b_k} Q_{(-k)}(C-b_k-y) \Bigg] \quad (38)$$

where the factor δ_k is given by (18).

As far as the values of P_{d_k} and P_{us_k} are concerned, they can be calculated via (20) and (21), respectively.

V. APPLICABILITY OF THE PROPOSED MODELS IN FUTURE LEO SDN/NFV ENABLED SATELLITE NETWORKS

A. SDN/NFV Enabled Satellite Network Architecture

Our considered SDN/NFV satellite network architecture is presented in Fig. 4. This is in line with the architecture proposed by the EC H2020 VITAL project [28], [29]. In Fig. 4, we depict a satellite network operator (SNO) enhanced with SDN/NFV infrastructure that enables multitenancy. SDN enables abstraction and modularity of the functions within the access network. This way, a hierarchical control architecture can be implemented, in which the high control layer controls lower layers through defining behaviors and enforcing policies, and without the need to know the specific implementation of the lower layers [30]. This requires a holistic view of the network at the higher control layer to be built on appropriate abstraction of lower layers via well-defined control interfaces. This is essential to enable programmable radio resource management (RRM) functions, such as the radio resource allocation and call admission control. On the other hand, the NFV technology allows the execution of control programs on general purpose computing/storage resources [31].

The SNO has multiple virtual SNOs (VSNOs) as its customers. Consequently, VSNOs offer satellite services to their customers without owing any physical infrastructure. In particular, the architecture consists of the following parts.

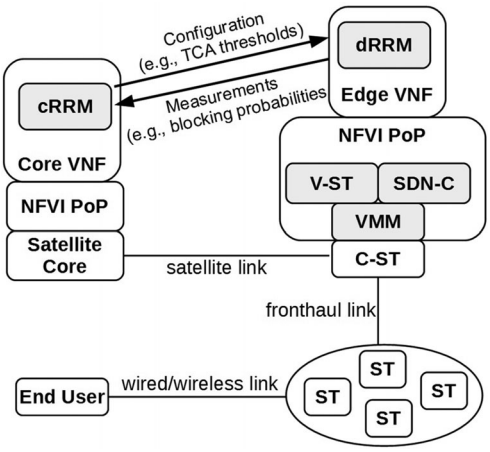

Fig. 5. Enabling SDN/NFV based radio resource management.

1) Various control and management systems, such as the network control center (NCC) and the network management center (NMC) (for simplicity not shown in Fig. 4).
2) Satellite core network, where the SNO at various locations has installed NFV infrastructure (NFVI) points of presence (PoPs). On top of the NFVI, different tenants (i.e., VSNO1 and VSNO2 in this example) can install and operate their own virtual network functions (VNFs), such as load balancers, firewalls, etc.
3) Satellite access network that consists of a cluster of SDN-enabled hubs, connected to the core network, and a distributed set of satellite terminals (STs), connected to the user equipment. Both, hubs and STs are part of the NFVI. As shown in Fig. 4, some STs can be multitenant, whereas others can be dedicated to a single VSNO.
4) A constellation of LEO satellites which connects hubs to STs.

B. Applicability of the Proposed Models

In this section, we demonstrate the applicability of our proposed models in SDN/NVF enabled satellite networks. As a specific example, consider the virtualization of the RRM function. One way to realize that is shown in Fig. 5 and is described below.

At the satellite core network level, the NFVI PoPs enable the execution of VNFs by the tenants (VSNOs). One such VNF could be a centralized RRM (cRRM) function that sets the configuration parameters, e.g., appropriate levels of QoS or CBP for VSNO's customers.

On the other hand, at the satellite access network level, there is a distributed set of STs, which form a centralized pool of ST resources (C-ST) that is owned and controlled by the SNO. To benefit from NFV, the C-ST functionality and services have been abstracted from the underlying infrastructure and virtualized (V-ST). The virtual machine monitor (VMM) manages the execution of V-STs. The NFVI PoP also includes an SDN controller that decides routes and configures the packet forwarding elements. On top of the NFVI, a VSNO can execute a number of edge VNFs, such as the distributed RRM (dRRM) function.

As shown in Fig. 5, the dRRM is logically connected to the cRRM. The cRRM sends to the dRRM various guidelines, configuration settings, and parameters. The cRRM determines the configuration parameters (e.g., call admission control thresholds) based on a number of objectives (e.g., QoS assurance for a particular service, acceptable handover failure probabilities, coverage requirements, capacity requirements, etc). For example, the cRRM can select a set of TCA policy thresholds, N_k, or FCR policy channel reservation parameters, CR_k, that can ensure certain target CBP for a particular service-class. The dRRM receives the configuration parameters and acts accordingly (e.g., rejects connection requests that do not conform to the specified requirements). Also, the dRRM sends (at regular intervals or when a predefined condition is met) to the cRRM various performance measurements and alarms, e.g., the dRRM may be configured to report the handover failure probabilities per service to the cRRM. If the reported measurements violate the objectives/performance constraints (e.g., QoS is below a predefined level or the handover failure probability for a particular service is too high), the cRRM will recalculate and send updated configuration parameters to the dRRM. For example, the dRRM may modify the CR_k parameters of the FCR policy in (23) and (24), so that a different P_{f_k} can be obtained in (27) for a particular service-class k. Similarly, the thresholds N_k of the TCA policy can be modified to reflect the desirable P_{b_k} and P_{f_k} in (37) and (38), respectively.

VI. EVALUATION

In this section, we present two application examples. In the first one, we provide analytical results of the CBP, the handover failure probability, the call dropping probability and the unsuccessful call probability for the proposed formulas of the TCA and the FCR policies. Analytical results are also compared to simulation results. In the second example, we consider only the TCA policy and show a case where oscillations may occur in the CBP and handover failure probabilities.

For the simulation of the LEO-MSS we adopt the Iridium parameters. The simulated network consists of $N = 7$ contiguous cells (a typical value, see e.g., [32], [33]). Extensive simulations have shown that a higher value of N does not affect our results. The subsatellite point speed is $V_{tr} = 26600$ km/h and the length of each cell is $L = 425$ km resulting in a maximum dwell time of a call in a cell equal to 57.5 s. MUs are uniformly distributed in the network of cells and new calls may arrive anywhere within the network. In addition, no distortion in the propagation links is considered.

Simulation results are derived via the Simscript III simulation language [34] and are mean values of 7 runs. In each run, twenty million calls are generated. Due to stabilization time, we exclude the blocking events of the first 3% of the generated calls. Confidence intervals of the results are found to be very small (less than two orders of magnitude) and are not presented in Figs. 6–10. Each run requires on

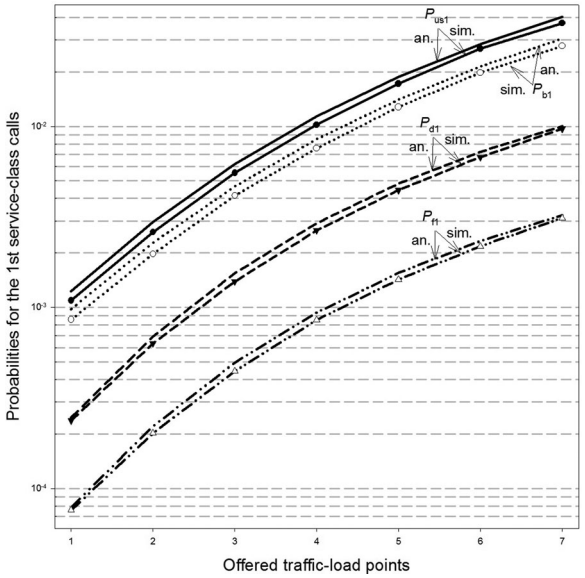

Fig. 6. TCA policy (1st set)—1st service-class.

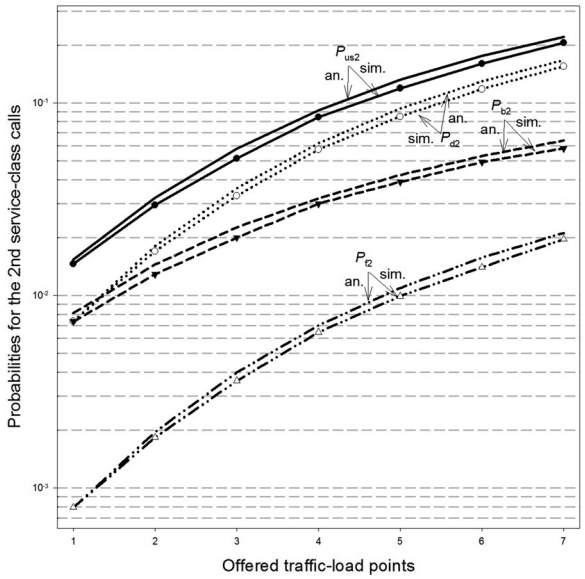

Fig. 7. TCA policy (1st set)—2nd service-class.

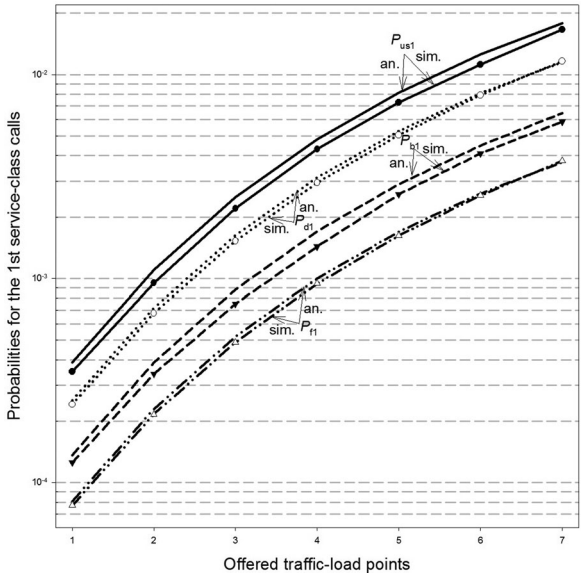

Fig. 8. TCA policy (2nd set)—1st service-class.

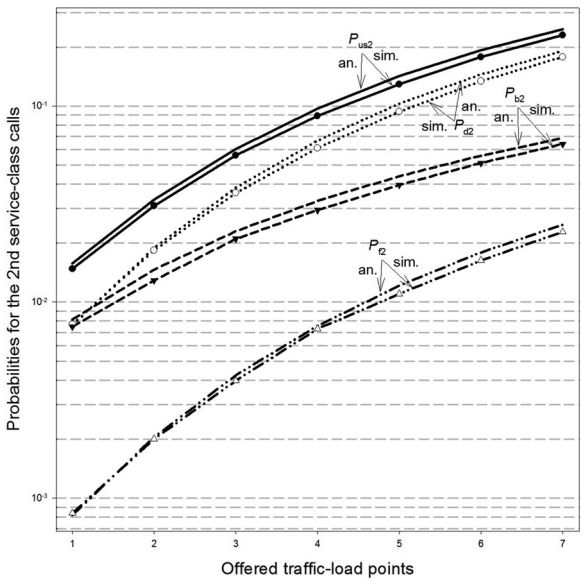

Fig. 9. TCA policy (2nd set)—2nd service-class.

average 16 and 19 min for the 1stand the 2nd example, respectively, in a computer of Intel(R) Core(TM) i5-2430M CPU @ 2.4 GHz and 4GB RAM. On the contrary, the analytical results are obtained in less than 1 s (on average for both examples).

In the first example, each cell has a capacity of $C = 40$ channels and accommodates Poisson arriving calls of two service-classes which require $b_1 = 1$ and $b_2 = 5$ channels, respectively. We further assume that $T_{d1} = 180$ s, $T_{d2} = 540$ s, while the offered traffic per cell is $\alpha_1 = 16$ erl and $\alpha_2 = 0.4$ erl. In the case of the TCA policy, we consider two sets of thresholds: 1) $N_1 = 30$, $N_2 = 3$ and 2) $N_1 = 38$, $N_2 = 3$ calls. In the case of the FCR policy, the FCR parameters for the new calls of each service-class are: $CR_1 = 4$ and $CR_2 = 0$ channels, respectively. This selection achieves CBP equalization among new calls of both service-classes, since $b_1 + CR_1 = b_2$.

In the x-axis of Figs. 6–10, the traffic loads α_1 and α_2 increase in steps of 1 and 0.1 erl, respectively. So, point 1 represents the offered traffic-load vector (α_1, α_2)=(16.0, 0.4), while point 7 refers to the vector (α_1, α_2)=(22.0, 1.0).

In Figs. 6–9, we consider the TCA policy. In Figs. 6–7, we consider the 1st set of thresholds and present the analytical/simulation results for the various performance measures for each service-class, respectively. In Figs. 8 and 9, we present the corresponding results for the 2nd set of thresholds. According to Figs. 6–9, we deduce that:

1) the analytical results obtained by the proposed formulas are close to the simulation results;
2) increasing the offered traffic-load results in the increase of all performance measures; and
3) increasing the value of N_1 from 30 to 38 calls, decreases/increases the CBP of the 1st/2nd service-class

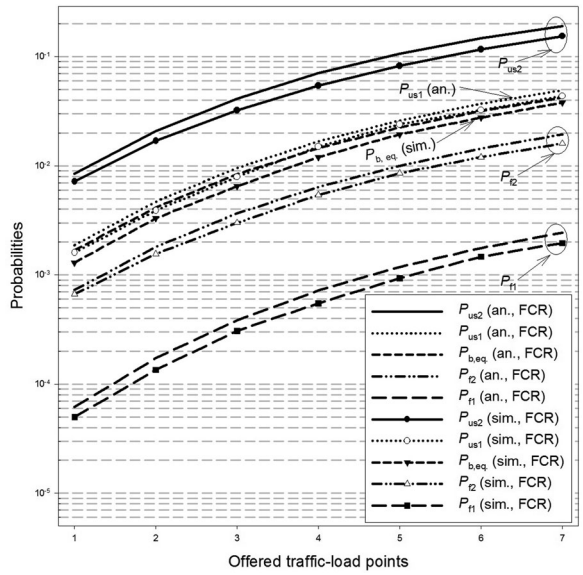

Fig. 10. FCR policy—Both service-classes.

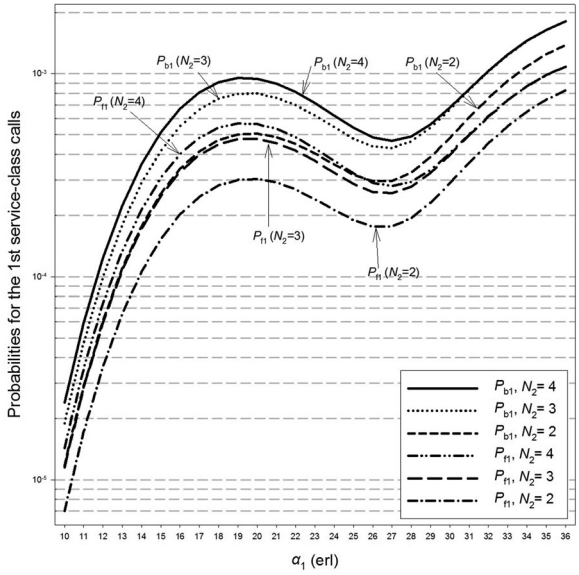

Fig. 11. Oscillations under the TCA policy.

calls, but increases the handover failure probabilities and the call dropping probabilities of both service-classes. This is intuitively expected since more new calls of the 1st service-class are allowed to enter the system.

In Fig. 10, we consider the FCR policy and present the analytical/simulation results for the various performance measures for both service-classes. The term $P_{b,eq}$ in Fig. 10 refers to the equalized CBP of both service-classes (achieved due to the selected FCR parameters). According to Fig. 10, we deduce that:

1) the accuracy obtained by the proposed formulas compared to simulation is highly satisfactory;
2) increasing the offered traffic-load results in the increase of all performance measures; and
3) the FCR policy fails to capture the behavior of the more complex TCA policy. This is because the FCR policy affects the number of channels reserved to benefit calls of a certain service-class while the TCA policy affects the number of calls that can be allowed in the system.

As a general and also final comment on Figs. 6–10, one may at first conclude that the analytical results are always slightly higher than the corresponding simulation results. However, this is only true for the current set of parameters, while it is not possible to provide "rules of thumb" on when analytical results will be above or below the corresponding simulation ones (e.g., Figs. 5a and b and 7a in [15] show the opposite behavior compared to Figs. 6–10 herein). Approximations such as (10) which is used for the determination of μ_k^{-1} or (18) which is proposed for the calculation of δ_k can affect (depending on the example) the analytical results compared to simulation.

In the second example, each cell has a capacity of $C = 100$ channels and accommodates Poisson arriving calls of two service-classes which require $b_1 = 1$ and $b_2 = 20$ channels, respectively. We assume that $T_{d1} = 180$ s, $T_{d2} = 540$ s, while the offered traffic per cell is $\alpha_1 = 10$ erl and $\alpha_2 = 1.0$ erl. We consider the TCA policy and three sets of thresholds: 1) $N_1 = 70, N_2 = 2, 2)$ $N_1 = 70, N_2 = 3$ and 3) $N_1 = 70$, $N_2 = 4$ calls.

Fig. 11 shows the analytical CBP and handover failure probabilities for the 1st class service-class and the three different sets of thresholds. For presentation purposes, we do not show simulation results whose form is similar. According to Fig. 11 and contrary to the first example, the increase of the offered traffic-load does not necessarily lead to an increase of CBP or handover failure probabilities, i.e., we see that oscillations can appear in the TCA policy. To intuitively explain such oscillations, consider an instant where a new call of the 1st service-class arrives in a cell and finds 20 available channels. In that case, the call is accepted and the cell has 19 available channels. If now a new call of the 2nd service-class arrives in the cell it will be blocked, leaving the 19 channels for calls (new or handover) of the 1st service-class. In such a case, an increase in α_1 will not lead to a CBP or handover failure probabilities increase. As α_1 continues to increase, the corresponding probabilities of the 1st service-class calls will increase until another block of 19 channels becomes available to 1st service-class calls. Such oscillations have not been studied in [15]–[17] and show that attention is needed when dimensioning a system, especially when calls of a service-class require much more bandwidth than others. Note that oscillations do not appear in the case of the 2nd service-class and, thus, we do not present the corresponding results. Slight oscillations can also appear for the 1st service-class calls in the case of the FCR policy, but only for small values of the FCR parameters and not when CBP equalization is required.

VII. CONCLUSION

In this paper, we concentrate on two different channel sharing policies, namely the fixed channel reservation and the threshold call admission policies and provide an

analytical framework for the efficient calculation of various performance measures in a LEO mobile satellite system with "satellite-fixed" cells. The proposed analytical formulas have low computational complexity compared to the methodologies already proposed in the literature, which are based on solving extremely large systems of linear global balance equations. The latter is a task that cannot be invoked in time efficient network planning and dimensioning procedures. Furthermore, we discuss the applicability of the policies in future LEO SDN/NFV enabled satellite networks.

APPENDIX A

Let $E_k(n_{hk})$ be the average number of times that a new service-class k call is successfully handed over during its lifetime in the system and $P(n_{hk})$ the corresponding probabilities of having $n_{hk} = 0, 1, 2, ...$ successful handovers. To determine $E_k(n_{hk})$ we work as follows:

$$P(n_{hk} = 0) = (1 - P_{h1,k}) + P_{h1,k}P_{f_k}. \tag{A1}$$

Equation (A1) refers to the probability of zero successful handovers. This is either because we don't have a handover from the source cell [this happens with probability $(1 - P_{h1,k})$] or because we have a handover with probability $P_{h1,k}$ but this is blocked with probability P_{f_k}.

On the same hand

$$P(n_{hk} = 1) = P_{h1,k}(1-P_{b_k})(1-P_{h2,k} + P_{h2,k}P_{f_k}). \tag{A2}$$

Equation (A2) refers to the probability of one successful handover. This is because the call is not blocked and we have one successful handover from the source cell to the first transit cell, expressed by $P_{h1,k}(1 - P_{b_k})$ "and either" we don't have a handover in the next transit cell (expressed by $1 - P_{h2,k}$) "or" we have a handover in the next transit cell but it is blocked with probability $P_{h2,k}P_{f_k}$.

Similarly

$$\begin{aligned} &P(n_{hk} = 2) \\ &= P_{h1,k}(1-P_{b_k})P_{h2,k}(1-P_{f_k})(1-P_{h2,k}+P_{h2,k}P_{f_k}). \end{aligned} \tag{A3}$$

Equation (A3) refers to the probability of two successful handovers. This is because the call is not blocked and we have one successful handover from the source cell to the first transit cell with probability $P_{h1,k}(1 - P_{b_k})$ and a second successful handover from the first to the second transit cell with probability $P_{h2,k}(1 - P_{f_k})$. The last term shows that we don't have a handover in the next transit cell (expressed by $1 - P_{h2,k}$) "or" we have a handover in the next transit cell, but it is blocked with probability $P_{h2,k}P_{f_k}$.

Similarly, for the case of $P(n_{hk} = 3)$ we have

$$\begin{aligned} &P(n_{hk} = 3) \\ &= P_{h1,k}(1-P_{b_k})\big(P_{h2,k}(1-P_{f_k})\big)^2(1-P_{h2,k}+P_{h2,k}P_{f_k}). \end{aligned} \tag{A4}$$

or generally for the case of $P(n_{hk} = i)$

$$\begin{aligned} &P(n_{hk} = i) \\ &= P_{h1,k}(1-P_{b_k})\big(P_{h2,k}(1-P_{f_k})\big)^{i-1}(1-P_{h2,k}+P_{h2,k}P_{f_k}). \end{aligned} \tag{A5}$$

Thus, based on (A5) and assuming that $Z = P_{h1,k}(1 - P_{b_k})(1 - P_{h2,k} + P_{h2,k}P_{f_k})$ and $x = P_{h2,k}(1 - P_{f_k})$ we have: $E_k(n_{hk}) = \sum_{i=1}^{\infty} i\,P(n_{hk} = i) = \sum_{i=1}^{\infty} i\,P_{h1,k}(1 - P_{b_k})\big(P_{h2,k}(1 - P_{f_k})\big)^{i-1}(1 - P_{h2,k} + P_{h2,k}P_{f_k}) = Z\sum_{i=1}^{\infty} i\big(P_{h2,k}(1 - P_{f_k})\big)^{i-1} = Z\sum_{i=1}^{\infty} ix^{i-1} = Z\frac{1}{(1-x)^2} \Rightarrow E_k(n_{hk}) = \frac{(1-P_{b_k})P_{h1,k}}{1-(1-P_{f_k})P_{h2,k}}$ which is (19).

APPENDIX B

By definition

$$q(j) = \sum_{\boldsymbol{n}\in\boldsymbol{\Omega}_j} P(\boldsymbol{n}) \tag{B1}$$

where $\boldsymbol{\Omega}_j$ is the set of states whereby exactly j channels are occupied by all in-service calls, i.e., $\boldsymbol{\Omega}_j = \{\boldsymbol{n} \in \boldsymbol{\Omega} : \boldsymbol{nb} = j\}$.

Since $j = \boldsymbol{nb} = \sum_{k=1}^{2K} n_k b_k$, (B1) can be written as follows:

$$jq(j) = \sum_{k=1}^{2K} b_k \sum_{\boldsymbol{n}\in\boldsymbol{\Omega}_j} n_k P(\boldsymbol{n}). \tag{B2}$$

To determine the $\sum_{\boldsymbol{n}\in\boldsymbol{\Omega}_j} n_k P(\boldsymbol{n})$ in (B2), we assume that LB exists between states $\boldsymbol{n}_k^-$, $\boldsymbol{n}$ and has the following form

$$\alpha_k(\boldsymbol{n}_k^-)P(\boldsymbol{n}_k^-) = n_k P(\boldsymbol{n}) \tag{B3}$$

where $\alpha_{k,}(\boldsymbol{n}_k^-) = \begin{cases} \lambda_k(\boldsymbol{n}_k^-)/\mu_k, k = 1, \ldots, K \\ \lambda_k(\boldsymbol{n}_{kh}^-)/\mu_k, k = K+1, \ldots, 2K \end{cases}$.

Summing both sides of (B3) over $\boldsymbol{\Omega}_j$ we have

$$\sum_{\boldsymbol{n}\in\boldsymbol{\Omega}_j} \alpha_k(\boldsymbol{n}_k^-)P(\boldsymbol{n}_k^-) = \sum_{\boldsymbol{n}\in\boldsymbol{\Omega}_j} n_k P(\boldsymbol{n}). \tag{B4}$$

The left-hand side of (B4) can be written as

$$\sum_{\boldsymbol{n}\in\boldsymbol{\Omega}_j} \alpha_k(\boldsymbol{n}_k^-)P(\boldsymbol{n}_k^-) = \alpha_k(j - b_k)q(j - b_k) \tag{B5}$$

where

$$\alpha_k(j - b_k) = \begin{cases} \alpha_k, \text{ for } j \le C - CR_k \\ 0, \text{ otherwise} \end{cases}. \tag{B6}$$

Based on (B4)–(B6), we write (B2) as (25).

REFERENCES

[1] Z. Sun
Satellite Networking–Principles and Protocols. 2nd ed., New york, NY, USA: Wiley, 2014.

[2] T. Li, H. Zhou, H. Luo, Q. Xu, and Y. Ye
Using SDN and NFV to implement satellite communication networks
Proc. Int. Conf. Netw. Netw. Appl., Hokkaido, Japan, Jul. 2016.

[3] B. Yang, Y. Wu, X. Chu, and G. Song
Seamless handover in software-defined satellite networking
IEEE Commun. Lett., vol. 20, no. 9, pp. 1768–1771, Sep. 2016.

[4] G. Maral, J. Restrepo, E. Del Re, R. Fantacci, and G. Giambene
Performance analysis for a guaranteed handover service in an LEO constellation with a "satellite-fixed cell" system
IEEE Trans. Veh. Technol., vol. 47, no. 4, pp. 1200–1214, Nov. 1998.

[5] J. Zhou, X. Ye, Y. Pan, F. Xiao, and L. Sun
Dynamic channel reservation scheme based on priorities in LEO satellite systems
J. Syst. Eng. Electron., vol. 26, no. 1, pp. 1–9, Feb. 2015.

[6] Z. Wang and P. T. Mathiopoulos
Analysis and performance evaluation of dynamic channel reservation techniques for LEO mobile satellite systems
Proc. IEEE VTC Spring, Rhodes, Greece, May 2001, pp. 2985–2989.

[7] L. Bouchatem, D. Gaiti, and G. Pujolle
TCRA: A time-based channel reservation scheme for handover requests in LEO satellite systems
Int. J. Satell. Commun. Netw., vol. 21, no. 3, pp. 227–240, May 2003.

[8] X. Wang and X. Wang
The research of channel reservation strategy in LEO satellite network
In *Proc. 11th IEEE Int. Conf. Dependable Autonomic Secure Comput.*, Chengdu, China, Dec. 2013, pp. 590–594.

[9] E. Papapetrou and F. N. Pavlidou
Analytic study of Doppler-based handover management in LEO satellite systems
IEEE Trans. Aerosp. Electron. Syst., vol. 51, no. 3, pp. 830–839, Jul. 2005.

[10] S. Karapantazis and F.-N. Pavlidou
Dynamic time-based handover management in LEO satellite systems
Electron. Lett., vol. 43, no. 5, pp. 57–58, Mar. 2007.

[11] L. Chen, Q. Guo, and H. Wang
A handover management scheme based on adaptive probabilistic resource reservation for multimedia LEO satellite networks
Proc. Int. Conf. Inf. Eng., Beidaihe, China, Aug. 2010, pp. 255–259.

[12] M. Liao, Y. Liu, H. Hu, and D. Yuan
Analysis of maximum traffic intensity under pre-set quality of service requirements in low earth orbit mobile satellite system for fix channel reservation with queueing handover scheme
IET Commun., vol. 9, no. 13, pp. 1575–1582, Aug. 2015.

[13] R. Musumpuka, T. Walingo, and MacGregor J. Smith
Performance analysis of correlated handover service in LEO mobile satellite systems
IEEE Commun. Lett., vol. 20, no. 11, pp. 2213–2216, Aug. 2016.

[14] Z. Wang, P. T. Mathiopoulos, and R. Schober
Performance analysis and improvement methods for channel resource management strategies of LEO-MSS with multiparty traffic
IEEE Trans. Veh. Tech., vol. 57, no. 6, pp. 3832–3842, Nov. 2008.

[15] Z. Wang, P. T. Mathiopoulos, and R. Schober
Channeling partitioning policies for multi-class traffic in LEO-MSS
IEEE Trans. Aerosp. Electron. Syst., vol. 45, no. 4, pp. 1320–1334, Oct. 2009.

[16] Z. Wang, D. Makrakis, and P. T. Mathiopoulos
Optimal channel partitioning and channel utilization for multi-class traffic in a LEO-MSS
IEEE Trans. Aerosp. Electron. Syst., vol. 46, no. 4, pp. 2102–2107, Oct. 2010.

[17] Z. Wang, D. Makrakis, and H. Mouftah
Performance analysis of threshold call admission policy for multi-class traffic in Low Earth Orbit Mobile Satellite Systems
Proc. 2nd Int. Conf. Adv. Satell. Space Commun., Athens, Greece, Jun. 2010.

[18] I. Moscholios, V. Vassilakis, J. Vardakas, and M. Logothetis
Call blocking probabilities of elastic and adaptive traffic with retrials
Proc. 8th Adv. Int. Conf. on Telecommun., Stuttgart, Germany, May 2012, pp. 44–52.

[19] I. Moscholios, M. Logothetis, and A. Boucouvalas
Blocking probabilities of elastic and adaptive calls in the Erlang multirate loss model under the threshold policy
Telecommun. Syst., vol. 62, is. 1, pp. 245–262, May 2016.

[20] M. Stasiak
Queuing systems for the Internet
IEICE Trans. Commun., vol. E99-B, no. 6, pp. 1234–1242, Jun. 2016.

[21] I. Moscholios, V. Vassilakis, M. Logothetis, and A. Boucouvalas
A probabilistic threshold-based bandwidth sharing policy for wireless multirate loss networks
IEEE Wireless Commun. Lett., vol. 5, no. 3, pp. 304–307, Jun. 2016.

[22] M. Glabowski, S. Hanczewski, and M. Stasiak
Modelling load balancing mechanisms in self-optimizing 4G mobile networks with elastic and adaptive traffic
IEICE Trans. Commun., vol. E99-B, no. 8, pp. 1718–1726, Aug. 2016.

[23] M. Benslama, W. Kiamouche, and H. Batatia
Connections Management Strategies in Satellite Cellular Networks, New York, NY, USA: Wiley, 2015.

[24] Del Re, E., R. Fantacci, and G. Giambene
Performance analysis of dynamic channel allocation technique for satellite mobile cellular networks
Int. J. Satell. Commun., vol. 12, no. 1, pp. 25–32, Jan. 1994.

[25] M. Stasiak, M. Glabowski, A. Wisniewski, and P. Zwierzykowski
Modeling and Dimensioning of Mobile Networks. New York, NY, USA: Wiley, 2011.

[26] J. Kaufman
Blocking in a shared resource environment
IEEE Trans. Commun., vol. 29, no. 10, pp. 1474–1481, Oct. 1981.

[27] J. Roberts
A service system with heterogeneous user requirements
Perform. Data Commun. syst. Appl., Amsterdam, The Netherlands, vol. 29, no. 10, pp. 423–431, 1981.

[28] R. Ferrús *et al.*
SDN/NFV-enabled satellite communications networks: Opportunities, scenarios and challenges
Phys. Commun., vol. 18, pp. 95–112, Mar. 2016.

[29] EC H2020 VITAL (VIrtualized hybrid satellite-TerrestriAl systems for resilient and fLexible future networks) project, [Online]. Available: www.ict-vital.eu/

[30] T. Chen, M. Matinmikko, X. Chen, X. Zhou, and P. Ahokangas
Software defined mobile networks: Concept, survey, and research directions
IEEE Commun. Mag., vol. 53, no. 11, pp. 126–133, Nov. 2015.

[31] ETSI GS NFV-MAN 001 (V1.1.1) "Network Function Virtualisation (NFV); Management and Orchestration
Dec. 2014.

[32] E. Del Re, R. Fantacci, and G. Giambenne
An efficient technique for dynamically allocating channels in satellite cellular networks
Proc. IEEE Globecom, Singapore, Nov. 1995, pp. 1624–1628.

[33] Z. Wang and P. T. Mathiopoulos
On the performance analysis of dynamic channel allocation with FIFO handover queueing in LEO-MSS
IEEE Trans. Commun., vol. 53, no. 9, pp. 1443–1446, Sep. 2005.

[34] Simscript III, [Online]. Available: http://www.simscript.com. Accessed on: Dec. 2017.

Ioannis D. Moscholios received the Dipl.-Eng. degree in electrical & computer engineering from the University of Patras, Patras, Greece, in 1999, the M.Sc. degree in spacecraft technology & satellite communications from the University College London, London, U.K., in 2000 and the Ph.D. degree in electrical & computer engineering from the University of Patras, in 2005.

He is currently an Assistant Professor with the Department of Informatics & Telecommunications, University of Peloponnese, Tripolis, Greece. He has authored or coauthored 140 papers in international journals/conferences. His research interests include teletraffic engineering, simulation and performance analysis of communication networks.

Dr. Moscholios was a Guest Editor in IET Communications, IET Networks, Mobile Information Systems and Image Processing and Communications. He was an Associate Editor in *IEICE Transactions on Communications* and in the TPC of IEEE ICC and Globecom. He is an IARIA Fellow and a member of the Technical Chamber of Greece.

Vassilios G. Vassilakis received the Ph.D. degree in electrical & computer engineering from the University of Patras, Patras, Greece, in 2011.

He is currently a Lecturer with the Department of Computer Science, University of York, York, U.K. From 2011 to 2013, he was with the Network Convergence Laboratory, University of Essex. In 2013, he joined the Institute for Communication Systems, University of Surrey, and conducted research on 5G wireless networks. After that, he was with the Computer Laboratory, University of Cambridge, where he conducted research on future Internet technologies. His main research interests include 5G wireless and mobile networks, network security, software-defined networks, and Internet of things. He has contributed to many UK, EU, and industry funded R&D projects.

Dr. Vassilakis was a Guest Editor in *IEICE Transactions on Communications*, *Elsevier Optical Switching & Networking*, and *IET Networks*, and for the TPC of IEEE ICC and IEEE GLOBECOM.

Nikos C. Sagias (SM'11) received the B.Sc. degree in physics from the Department of Physics, University of Athens (UoA), Athens, Greece, in 1998 and the M.Sc. and Ph.D. degrees in telecommunications engineering from UoA, in 2000 and 2005, respectively.

He is currently an Associate Professor with the Department of Informatics & Telecommunications, University of Peloponnese, Tripolis, Greece. In his record, he has authored or coauthored 50 papers in prestigious international journals and more than 30 in the proceedings of world recognized conferences. His research interests include digital communications, and more specifically MIMO and cooperative systems, fading channels, mobile and satellite communications, optical wireless systems, and communication theory issues.

Dr. Sagias is a TPC member for various IEEE conferences (ICC, GLOBECOM, VTC, etc), while during 2009–2014 he was an Associate Editor for the IEEE TRANSACTIONS ON WIRELESS COMMUNICATIONS. He is a member of the IEEE Communications Society.

Michael D. Logothetis (SM'08) received the Dipl.-Eng. degree and Doctorate degree in electrical engineering, both from the University of Patras, Patras, Greece, in 1981 and 1990, respectively.

From 1991 to 1992, he was a Research Associate with NTT's Telecommunication Networks Laboratories, Tokyo, Japan. Afterwards, he was a Lecturer with the Department of ECE, University of Patras, where he was a Full Professor. He has authored or coauthored more than 200 conference/journal papers. His research interests include teletraffic theory, simulation and performance optimization of telecommunications networks.

Dr. Logothetis is a Guest Editor in *Mediterranean Journal of Electronics and Communications*, *Mediterranean Journal of Computers and Networks*, *IET Circuits, Devices & Systems*, *IET Networks and Ubiquitous Computing and Communication Journal*. He is a member of the IARIA (Fellow), IEICE, FITCE and the Technical Chamber of Greece.